2010 IEEE International Conference of Electron Devices and Solid-State Circuits (EDSSC)

Modelling and Stability Analysis of Coupled Inductor Bidirectional DC-DC Converter

Narasimharaju.B.L
Department of Electrical Engineering
Indian Institute of Technology
Roorkee-247 667, India
E-mail: *narasimharaju.bl@gmail.com*

S. P. Dubey
Department of Electrical Engineering
Indian Institute of Technology
Roorkee-247 667, India
E-mail: *spdubfee@iitr.ernet.in*

S. P. Singh
Department of Electrical Engineering
Indian Institute of Technology
Roorkee-247 667, India
Email: *spseefee@iitr.ernet.in*

Abstract— **This paper emphasizes on the small-signal behavior and stability analysis of bidirectional DC to DC converter. The bidirectional current capability of the switch eliminates the discontinuous conduction mode which leads to a simple analytic description of the switching converter. The small-signal model is considered to design the control parameters. The transient, stability analyses and closed loop regulation have been studied extensively. The closed loop model has also been developed and simulated using Matlab/Simulink environment. The closed loop performances of the converter are evaluated for wide range of load conditions.**

Keywords- Bidirectional converter; Coupled inductor; State Space (SS) Modeling ; Satbility;

I. Introduction

The inherent switching operation of power electronic converters results in the circuit components being connected together in periodically changing configurations, each configuration being described by a separate set of equations. The transient analysis and control design for converters is therefore difficult, since a number of equations must be solved in sequence. The technique of averaging provides a solution to this problem. The State-Space (SS) averaging [1, 2, 3] has proven, in the past, to be very popular analysis technique for PWM power conversion circuits. Middlebroke have been discussed the detailed SS technique approach in [1]. Use of this approach has been made in deriving converter models to assess small-signal [1, 3] and large-signal performances [7, 8]. Small-signal models provide a means of assessing local stability and are of great importance in the design of the feedback loop in regulated converters. In this paper a state-space modeling analysis of coupled inductor bidirectional DC (BDC) converter. The detailed operation and analysis is reported in [9]. This paper, presents five sections which includes section-I, section-II discuses modeling of the converter, section-III provides controller modeling and stability analysis; section-IV emphasizes on closed loop implementation in Simulink, and in section-V discusses the concluding remarks.

II. Small Signal Modeling of the Converter System

BDC technology has been in the reasonably development stages for DC-DC conversion with high efficiency and reduced stress on switches. Fig.1 depicts the proposed coupled inductor BDC converter, for which, small-signal modeling and control behavior has been analyzed extensively. All switches and diodes are assumed to be ideal, therefore no parasitics effects. Here, two state variables, inductor current $i_L(t)=X1(t)$, and capacitor voltage $v_C(t)=X2(t)$ are considered. Due to the bidirectional current ability, discontinuous current does not takes place. Therefore, in continuous conduction mode the converter can be represented by two piecewise-linear vector differential equations as follows:

$$\dot{X} = A_{ON} X + B_{ON} U \quad for \quad 0 < t \le \delta T \tag{1}$$

$$\dot{X} = A_{OFF} X + B_{OFF} U \quad for \quad \delta T \le t < T \tag{2}$$

The output equations are described as

$$Y = C_{ON} X + D_{ON} U \quad for \quad 0 < t \le \delta T \tag{3}$$

$$Y = C_{OFF} X + D_{OFF} U \quad for \quad \delta T \le t < T$$

Where, Y is the output vector, T is the switching frequency and δ is the duty cycle for switch (S1) and its complement is the duty cycle (δ^1) for switch (S2).

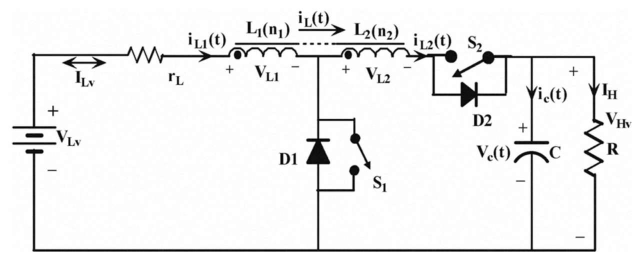

Fig. 1. Proposed Bidirectional DC-DC converter and its equivalent circuits

Where, $X = \begin{bmatrix} i_L(t) \\ v_C(t) \end{bmatrix} \quad \dot{X} = \begin{bmatrix} \frac{di_L}{dt} \\ \frac{dv_C}{dt} \end{bmatrix} \quad U = \begin{bmatrix} V_{LV} \\ I_H \end{bmatrix}$

$$A_{ON} = \begin{bmatrix} \frac{-r_L}{L} & 0 \\ 0 & \frac{-1}{RC} \end{bmatrix} \quad B_{ON} = \begin{bmatrix} \frac{1}{L} & 0 \\ 0 & \frac{1}{C} \end{bmatrix}$$

$$C_{ON} = \begin{bmatrix} 0 & 1 \end{bmatrix} \quad C_{OFF} = \begin{bmatrix} 0 & 1 \end{bmatrix} \quad D_{ON} = D_{OFF} = \begin{bmatrix} 0 \end{bmatrix}$$

978-1-4244-9996-0/10/$26.00 ©2010 IEEE

$$A_{OFF}=\begin{bmatrix} \frac{-r_L}{L(1+N)} & \frac{-1}{L(1+N)} \\ \frac{-1}{C} & \frac{-1}{RC} \end{bmatrix} \quad B_{OFF}=\begin{bmatrix} \frac{1}{L(N+1)} & 0 \\ 0 & \frac{1}{C} \end{bmatrix}$$

As shown in figure.1, $N=\frac{n_2}{n_1}$ is the turn's ratio of the coupled inductor (L).

$$A=\begin{bmatrix} t1 & t2 \\ t3 & t4 \end{bmatrix} \quad B=\begin{bmatrix} t5 & 0 \\ 0 & t6 \end{bmatrix} \qquad (5)$$

Since the duty ratio control appears within the B matrix of the averaged model rather than as an element in the input vector. The averaged model is therefore time varying and difficult to solve. However, the above difficulty can be overcome by small signal linearization. Using the small-signal assumptions for ac perturbations, after separating the steady-state DC quantities, and the second order non-linear terms which are smaller in compared to the first order ac-terms can be neglected. Therefore, the small-signal dynamic model [1-3] of the converter is described by

$$\dot{\tilde{x}}=A\tilde{x}+B\tilde{u}+E\tilde{\delta} \quad \tilde{y}=C^T\tilde{x}+F\tilde{\delta} \qquad (6)$$

Where, $A=A_{ON}\,\delta+A_{OFF}\,\delta^1 \quad B=B_{ON}\,\delta+B_{OFF}\,\delta^1$

$C=C_{ON}\,\delta+C_{OFF}\,\delta^1 \quad \delta^1=1-\delta$

$E=(A_{ON}-A_{OFF})X+(B_{ON}-B_{OFF})U \quad F=(C^T{}_{ON}-C^T{}_{OFF})X$ and $\tilde{x}\ \ \tilde{u}\ \ \tilde{\delta}\ \ \tilde{y}$ are the small perturbations of the state vector, input vector, duty cycle and output vector respectively.

$$E=\begin{bmatrix} t7 & t8 \\ t9 & 0 \end{bmatrix}\begin{bmatrix} i_L(t) \\ v_C(t) \end{bmatrix}+\begin{bmatrix} t10 \\ 0 \end{bmatrix}\begin{bmatrix} V_{LV} \\ I_H \end{bmatrix} \quad F=0 \qquad (7)$$

The coefficients of matrix A, B, and E are described as in table-I. The perturbed SS description is nonlinear owing to the presence of the product of the two time dependent quantities $\tilde{x}$ *and* $\tilde{\delta}$. Equation.(6) represent the two-state small signal low frequency model of the converter working in continuous conduction mode. Using (6) and table-I, the small-signal dynamic model of the BDC converter in boost mode is expressed as follows;

$$\frac{d\tilde{i}_L(t)}{dt}=t1*\tilde{i}_L(t)+t2*\tilde{V}_C(t)+t5*\tilde{V}_{LV}(t)+[t7*I_L(t)+t8*V_C(t)+t10*V_{LV}]\tilde{\delta} \qquad (8)$$

$$\frac{d\tilde{V}_C(t)}{dt}=t6*\tilde{I}_H+t3*\tilde{i}_L(t)+t4*\tilde{V}_C(t)+[t9*I_L(t)]\tilde{\delta} \qquad (9)$$

The block diagram was used in Simulink to examine the characteristics of the model and aid the design of the controller.

TABLE-I MATRIX COEFFICIENTS OF BDC STATE SPACE MODEL

MATRIX A	MATRIX B
$t1=\frac{-(N\delta+1)r_L}{L(1+N)}$, $t2=\frac{-(1-\delta)}{L(1+N)}$	$t5=\frac{(N\delta+1)}{L(N+1)}$
$t3=\frac{(1-\delta)}{C}$, $t4=\frac{-1}{RC}$	$t6=\frac{1}{C}$
MATRIX E	
$t7=\frac{-Nr_L}{L(1+N)}$, $t8=\frac{1}{L(1+N)}$, $t9=\frac{1}{C}$, $t10=\frac{N}{L(N+1)}$	

Equation.(8) and (9) are also valid for the buck operation by simply replacing the δ by δ^1 and vice versa, I_H (DC bus high voltage side current) by I_{LV} (Battery charging current) and V_{LV} (Battery voltage) by V_{HV} (DC bus high voltage $V_C(t)$). By using (8) and (9), block diagram model of small-signal equations may be constructed relating both the control and input to the inductor current and capacitor voltage as shown in Fig.2.

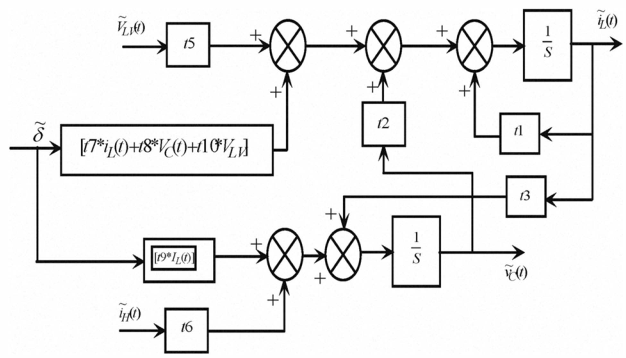

Fig.2. Small-signal model proposed converter

In order to regulate the output voltage, by applying Laplace transform, and setting $\tilde{i}_H(s)=0 \ \tilde{V}_{LV}(s)=0$ in (8) and (9), control to output transfer function is developed as

$$G_{vd}=\frac{\tilde{V}_C(t)}{\tilde{\delta}}=\frac{m(s-m1)}{S^2+S*t4-m2} \qquad (10)$$

Where, $m1=\frac{t3*[t7*I_L(t)+t8*V_C(t)+t10*V_{LV}]}{t9*I_L(t)(1-t1)}$

$m2=\frac{t3}{1-t1} \quad m=t9*I_L(t)$

III. CONTROLLER MODELING AND STABILITY ANALYSIS

To design effective compensator, it is necessary to have accurate small signal models of the plant. Thus, fig.3 illustrates the small-signal model of the convert with voltage controller. The designs of the controller parameters are undertaken in the frequency domain, and bode plots are used throughout the design process. The controller $G_c(S)$ used for the proposed converter is a combination of PI and lag- lead compensator given by

$$G_c=\frac{K(S+\tau_z{}^{-1})^2}{S^2+S*\tau_p{}^{-1}} \qquad (11)$$

Where τ_Z^{-1} *and* τ_P^{-1} is the zero and pole frequencies of the controller.

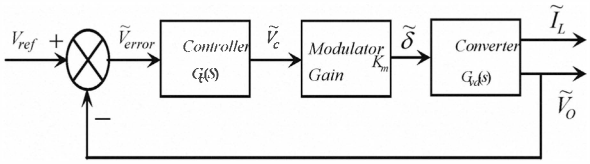

Fig.3 Closed loop system with voltage mode control of the converter

This controller is chosen to have an integral characteristic at low frequency in order to ensure zero steady-state error. A compensation term is added at higher frequency to provide a satisfactory crossover frequency and stability margin. The averaged models are typically accurate up to around one-third of the switching frequency, usually the value of 0-dB cross over frequency is lower than one-third of the switching frequency. Here, the controller is designed to achieve a crossover frequency to one-tenth the switching frequency (i.e. 5 kHz). The two zeros are placed at 10krad/sec, and high frequency pole is placed at 60krad/sec, approximately twice the target crossover frequency. The final selection of forward gain (K) is made by comparing the transient performances of the closed loop step references for different gains as illustrated in figure.5. Therefore, to achieve fast response with less overshoot, the value of forward gain (K) is chosen to be 0.1 and 0.95 for boost and buck mode operation respectively. The open loop transfer function of the converter system is given by

$$G_{OL} = G_{Vd} G_C K_m = \frac{m(s-ml)}{(S^2+S*t4-m2)} * \frac{K(s+\tau_Z^{-1})^2}{S^2+S*\tau_P^{-1}} \qquad (12)$$

The closed loop transfer function of the converter from reference (V_{ref}) to output (V_O) is given by

$$G_{CL} = \frac{G_{OL}}{(1+G_{OL})} \qquad (13)$$

In order to authenticate the model of the proposed BDC converter and control technique, specifications and design values are obtained [9] as described in table-II.

TABLE-II DATA FOR THE PROPOSED COUPLED BDC CONVERTER

Converter Specifications		
Parameter	**Boost (LV to HV)**	**Buck (HV to LV)**
Input voltage	V_{LV}=24±20%	V_{HV}=200±20%
Output voltage	V_{HV}= 200 V	V_{LV}=24V
ΔVo (Ripple)	≤0.5%	≤0.5%
Output Power	400 Watt	384 Watt
Output Current	2A	16A
Switching Frequency		50 kHz
Turns Ratio		2
Converter Designed/used Values		
Duty Cycles	Switch (S1) δ=0.71, Switch (S2) δ[1]=1- δ	
Inductors	L_1=20μH, L_2=200μH, M=98μH	
Resistors	R_{HV}=100 Ω, R_{LV}=1.44 Ω, r_L=0.001Ω,	
Capacitors	C=10μF,	

Transient and stability analysis of the converter system with voltage mode control has been synthesized using Matlab simulation. The comparative performances of the controllers in boost and buck mode as illustrated in fig.4. Thus, for best chosen controller's performance, converter system in both open loop and closed loop are analyzed. Fig.5 illustrates frequency responses of open loop and closed loop converter system in boost and buck mode. Fig.6 illustrates the closed loop unit step performances of the converter system.

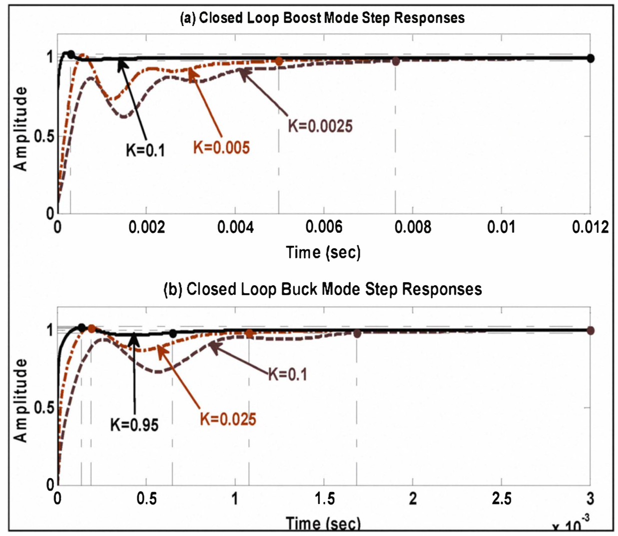

Fig.4. Comparative performances of converter system for different gains

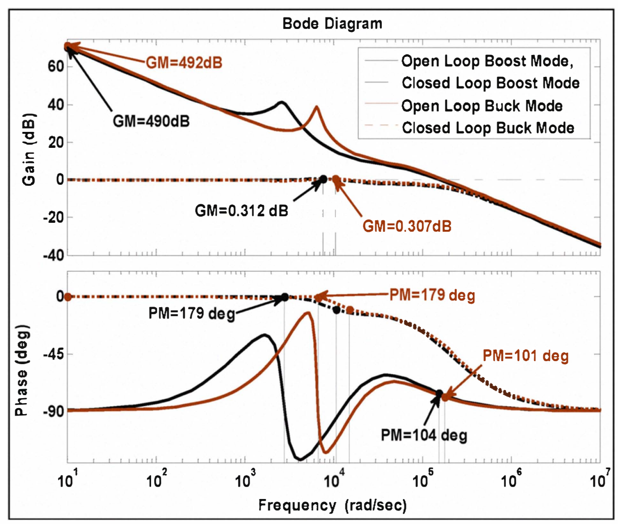

Fig.5. Frequency responses of open loop and closed loop converter system

IV. CLOSED LOOP IMPLEMENTATION IN SIMULINK

The voltage controller increases the immunity of the converter output voltage to changes in the input voltage and load current, therefore, the effect of these can be studied. Best among the tuned controller parameter is used for the converter system, The Simulink model of the BDC converter with voltage mode control has been developed as depicted in fig.8.

Thus, the performance analysis in closed loop has been evaluated extensively. Fig.8 and fig.9 illustrates the closed loop performances of the converter for various load conditions. The voltage controller increases the immunity of the converter output voltage to changes in the input voltage and load current. Here in, the load regulations under wide range of load conditions have been made extensively. Fig.8 depicts the effect of step load change from full load to quarter load is observed at 0.0075sec (0.5A) for boost mode, and at 0.0225 sec (6A) for buck mode respectively. Fig.9 depicts the effect of step load change from 20%full load(0.4A) to twice the full load is observed at 0.0075sec (4A) for boost mode, and from 31.25% full load(5A) to twice the full load at 0.0225 sec (32A) for buck mode respectively. Thus, it justifies the excellent load regulation in both modes of operation.

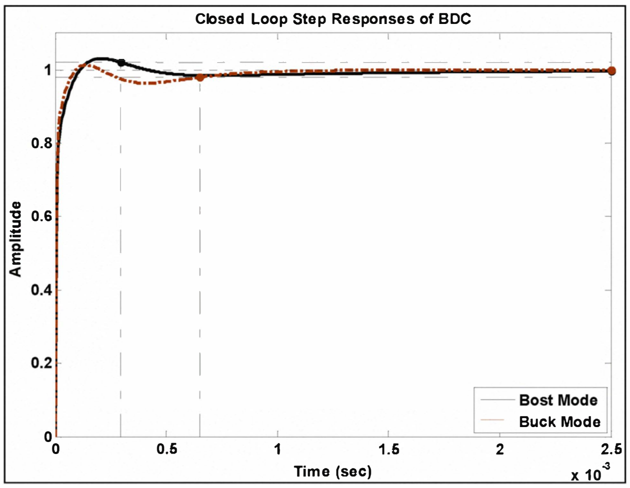

Fig.6. Closed loop unit step performances in converter system

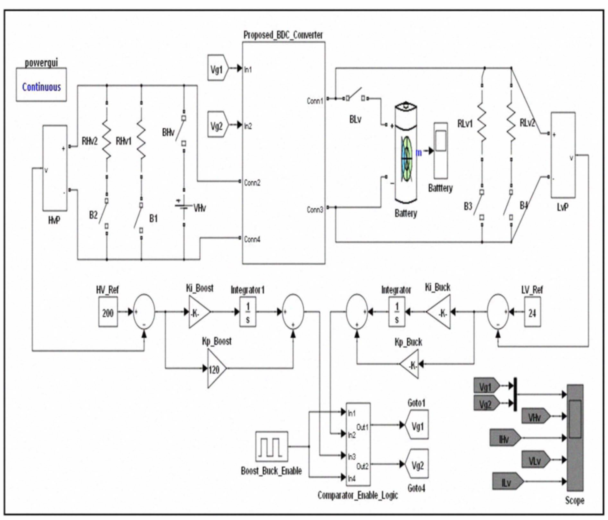

Fig. 7 Closed loop Simulink model of the bidirectional DC-DC converter

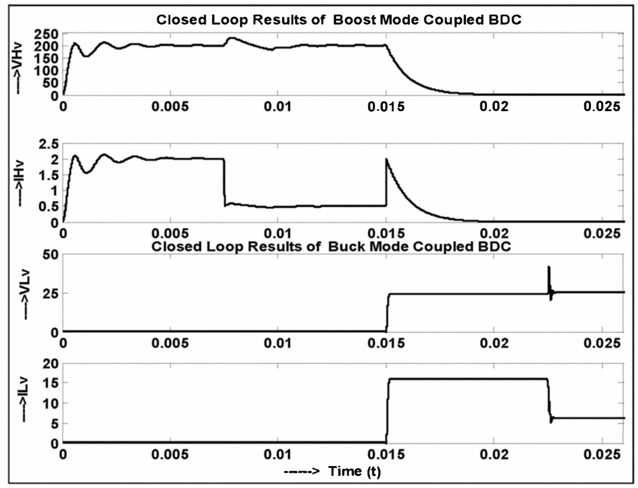

Fig.8 Closed loop performances for different step load changes from full load to light load

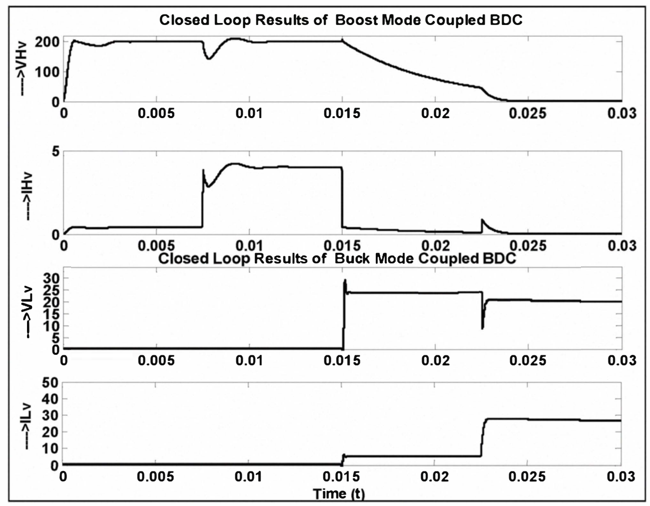

Fig.9 Closed loop performances for different step load changes from light load to overload full load

V. Conclusion

The detailed small-signal modeling of BDC converter and voltage mode controller is presented in this paper. The closed stability analysis of the converter has been extensively studied and the results show that significant improvements in transient responses, and in steady state conditions using voltage mode controller. Also, it was shown that the converter output voltage could be satisfactorily controlled by the use of single feedback loop of output voltage. The BDC converter with voltage mode control has been developed Simulink environment. Thus, the closed loop regulation is obtained for wide range of load conditions which show the excellent performances of PI controller. The simulation results show close agreement with the theatrical predictions and analysis.

VI. REFERENCES

[1] R.D Middlebrood and S. Cuk, "A general unified approach to modeling switching converter power supplies," in Proc. of IEEE PESC-76 Record, pp.73-86, 1976

[2] R.D Middlebrook, S. Cuk and W. Behen, "A new battery charger/discharger converter", in Proc. of IEEE PESC-78 Record, pp.251-55, 1978.

[3] S.P.Hsu, A.Brown, L.Rensink and R.D.Middlebrook, "Modeling and analysis of switching DC-DC converters in constant frequency current control mode", IEEE PESC-79 Record, pp. 169-86, 1979.

[4] Daniel M. Mitchell, "An analytical investigation of current injected control for constant frequency switching regulators," IEEE Trans on Power Electronics, vol.PE-1, July 1986, pp.167-74,

[5] A. Cape1, "A bidirectional high power cell using large signal feedback control with maximum current conduction control for space applications," IEEE PESC-86 Record, pp. 684-95, 1986.

[6] S.S Kelkar, "A computer aided design and simulation tool for switching converters", IEEE PESC-87 Record, pp. 3-12, 1987.

[7] D. Maksimovic and S. Cuk, "A General Approach to Synthesis and Analysis of Quasi-Resonant Converters", in IEEE Trans. on Power Electronics, Vol 6, No.1, Jan. 1991, pp. 127-140,.

[8] C. K. Tse and K. M. Adams, "A nonlinear large signal feed forward-feedback control for DC-DC converters,'' in Conf. Record. IEEE PESC-91, pp.722-729, 1991.

[9] Narasimharaju .B.L, S.P.Dubey, S.P.Singh, "Performance Analysis of a Coupled Inductor Bidirectional DC to DC Converter", Record of 4Th International Conference CERA2009, pp. 26 (1)-26(5), Feb 2010.